Received: 9 June 2023 | Revised: 6 August 2023 | Accepted: 7 August 2023

DOI: 10.1111/mmi.15143

RESEARCH ARTICLE

WILEY

In *Salmonella enterica*, the pathogenicity island 2 (SPI-2) regulator PagR regulates its own expression and the expression of a five-gene operon that encodes transketolase C

Anastacia R. Parks | **Regan D. McCormick** | **Jordan A. Byrne** | **Jorge C. Escalante-Semerena**

Department of Microbiology, University of Georgia, Athens, Georgia, USA

Correspondence
Jorge C. Escalante-Semerena, Department of Microbiology, University of Georgia, 212C Biological Sciences Building, 120 Cedar Street, Athens, Georgia 30602, USA.
Email: jcescala@uga.edu

Present address
Anastacia R. Parks, Department of Microbiology and Immunobiology, Harvard Medical School, Boston, Massachusetts, USA
Jordan A. Byrne, Molecular, Cellular, and Developmental Biology, University of Michigan, Ann Arbor, Michigan, USA

Funding information
National Institute of General Medical Sciences, Grant/Award Number: R35-GM130399

Abstract

The enteropathogen *Salmonella enterica* subsp. *enterica* sv. Typhimurium str. LT2 (hereafter *S.* Typhimurium) utilizes a cluster of genes encoded within the pathogenicity island 2 (SPI-2) of its genome to proliferate inside macrophages. The expression of SPI-2 is controlled by a complex network of transcriptional regulators and environmental cues, which now include a recently characterized DNA-binding protein named PagR. Growth of *S.* Typhimurium in low-phosphate, low-magnesium medium mimics conditions inside macrophages. Under such conditions, PagR ensures SPI-2 induction by upregulating the transcription of *slyA*, which encodes a known activator of SPI-2. Here, we report that PagR represses the expression of a divergently transcribed polycistronic operon that encodes the two subunits of transketolase TktC (i.e., *tktD*, *tktE*) of this bacterium. Transketolases contribute to the nonredox rearrangements of phosphorylated sugars of the pentose phosphate pathway, which provide building blocks for amino acids, nucleotides, cofactors, etc. We also demonstrate that PagR represses the expression of its own gene and define two PagR-binding sites between *stm2344* and *pagR*.

KEYWORDS
pagR gene expression, PagR protein, pentose phosphate pathway, *Salmonella* pathogenesis, *tktDE* expression, transcriptional regulation, transketolase

1 | INTRODUCTION

Transketolases are well-characterized enzymes that catalyze the nonoxidative transfer of a C2 unit from a ketose to an aldose, shortening the ketose by two carbons and lengthening the aldose by two carbons (Schneider & Lindqvist, 1998). Transketolases use thiamine pyrophosphate (TPP) as cofactor, whose ylid carbanion triggers a nucleophilic attack on the carbonyl group of the ketose. The addition product cleaves in a retro-aldol like reaction and the resulting enamine adds to the carbonyl group of the aldose. Elimination of the TPP ylid carbanion yields the final ketose product. Transketolase-catalyzed reactions are critical in processes such as the nonoxidative branch of the pentose phosphate pathway (nonoxPPP) (Stincone et al., 2015) and the Calvin–Benson–Bassham (CBB) cycle (Raines, 2003). Up until recently, the genome of *S.* Typhimurium was thought to encode only two transketolases, TktA and TktB. During the analysis of the genomic context of the *pagR* gene (locus tag *stm2345*), we noticed that *pagR* was transcribed divergently from a set of genes encoding a putative sugar transporter (*stm2342*, *stm2343*, *stm2344*) and two genes (*tktD*=*stm2341* and

Anastacia R. Parks and Regan D. McCormick contributed equally to this work.

 © 2023 John Wiley & Sons Ltd.

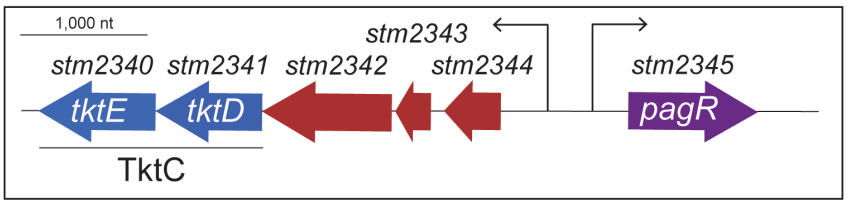


FIGURE 1 Genomic context of the *pagR* and *tktD*, *tktE* genes. PagR activates the transcription of the five-gene operon shown in the figure. The genes encoding the TktC transketolase are the most promoter-distal genes of the operon. *tktD* = 953 nt, *tktE* = 830 nt, *stm2342* = 1391 nt, *stm2343* = 272 nt, *stm2344* = 443 nt, *pagR* = 1019 nt. At present, the location of the promoters is hypothetical. The operon spans the region from 2,257,129 to 2454, 101 nt (i.e., 3028 nt) of the *Salmonella* Typhimurium chromosome. *pagR* spans the region from 2,457,382 to 2,458,401 nt. All genes are at scale.

tktE = *stm2340*) encoding the subunits of transketolase C (TktC, Figure 1).

TktC was recently characterized as an isozyme of transketolase A and transketolase B (Shaw et al., 2018). The TktA and TktB transketolases are housekeeping enzymes involved in the non-oxPPP. The reversibility of reactions catalyzed by transketolase enzymes involved in the non-oxPPP allows the production of intermediate compounds to meet metabolic demands of the cell through the diversion of metabolites to other pathways such as replenishment of glycolysis intermediates, or to provide building blocks for the biosynthesis of aromatic amino acids, nucleotides, or lipopolysaccharides (Stincone et al., 2015).

PagR is a transcriptional regulator that has recently been shown to indirectly induce the expression of SPI-2 through *slyA*, which is important for *S*. Typhimurium replication in macrophages and pathogenicity in mice (Jiang et al., 2020). PagR is annotated as a LacI/GalR family regulator, and its amino acid sequence contains the N-terminal helix-turn-helix motif characteristic of this family (Figure S1). In this paper, we show that (i) PagR regulates the expression of the divergently transcribed *tktDE* genes that encode the subunits of the TktC transketolase of this bacterium under conditions previously described (Jiang et al., 2020) and under conditions described in this report; (ii); PagR represses the expression of its own gene; and (iii); PagR directly binds the promoter region between *stm2344* and *pagR*, protecting two discreet binding sites.

2 | RESULTS AND DISCUSSION

2.1 | A *S*. Typhimurium Δ*pagR* strain fails to grow with succinate as a sole carbon and energy source

We probed for areas of *S*. Typhimurium metabolism that might be regulated by PagR. To this end, we tested the ability of a *S*. Typhimurium *pagR1*::*kan*$^+$ strain to catabolize various carbon sources. During this screen, we observed that a *pagR1*::*kan*$^+$ strain (JE21566) failed to grow with succinate was the sole carbon and energy source (Figure 2a, gray triangles vs. red circles). The observed phenotype was solely due to the lack of PagR, since we restored growth to the rate and density of the *pagR*$^+$ strain by ectopically expressing the *pagR*$^+$ allele (Figure 2a, dark green triangles). Surprisingly, we also corrected the growth phenotype by deleting the *tktD* and *tktE* genes encoding the two subunits of the TktC transketolase (*tktDE1*::*cat*$^+$, Figure 2a, blue squares). The latter was a notable result because the correction of the phenotype was as efficient as the ectopic expression of *pagR*$^+$. Likewise, the ectopic expression of the *tktDE*$^+$ genes repressed growth (Figure 2b, magenta squares), mimicking the growth behavior of a *pagR1*::*kan*$^+$ strain (Figure 2b, gray triangles). To investigate whether the observed phenotype was a result of excess transketolase activity, we expressed the other two *S*. Typhimurium transketolases in the *pagR1*::*kan*$^+$ *tktDE1*::*cat*$^+$ strain and monitored cell growth. Neither the ectopic expression of *tktA*$^+$ nor *tktB*$^+$ repressed the growth of the *pagR1*::*kan*$^+$ *tktDE1*::*cat*$^+$ strain like the overexpression of *tktDE*$^+$ did (Figure 2b, light green squares and yellow squares vs. magenta squares). Rather, the ectopic expression of *tktA*$^+$ and *tktB*$^+$ improved growth relative to the vector control. These data indicated that either the physiological role or the activity of TktC may be somehow different than that TktA and TktB in the cell during growth with succinate as the sole source of carbon and energy.

2.2 | PagR represses the expression of the operon containing *tktDE*, and its own gene

Given the proximity of *pagR* to the cluster containing the *tktD and tktE* genes (Figure 1) and the data presented in Figure 2, we investigated the possibility that PagR controlled the expression of the operon containing *tktD* and *tktE*. We isolated RNA from three strains, namely *pagR*$^+$/vector, *pagR1*::*kan*$^+$/vector, and *pagR1*::*kan*$^+$/pPagR, and quantified the amount of *stm2343*, *tktD*, and *tktE* mRNA using RT-qPCR. For this purpose, cells were grown on lysogeny broth (LB) plus ampicillin, L-(+)-arabinose (100 μM) and RNA isolated from cultures at an OD_{600} of 0.5. As shown in Figure 3a, expression of *stm2343*, *tktD*, and *tktE* increased ~10 fold in the *pagR1*::*kan*$^+$/vector strain (red bars) when compared to the *pagR*$^+$/vector and the *pagR1*::*kan*$^+$/pPagR strains (black and blue bars, respectively).

To assess whether PagR regulated its own expression, we constructed a *lacZY* transcriptional fusion with the chromosomal *pagR* gene and assayed β-galactosidase activity with and without ectopic expression of *pagR*. Cells were grown to an OD_{600} of ~0.5 in LB

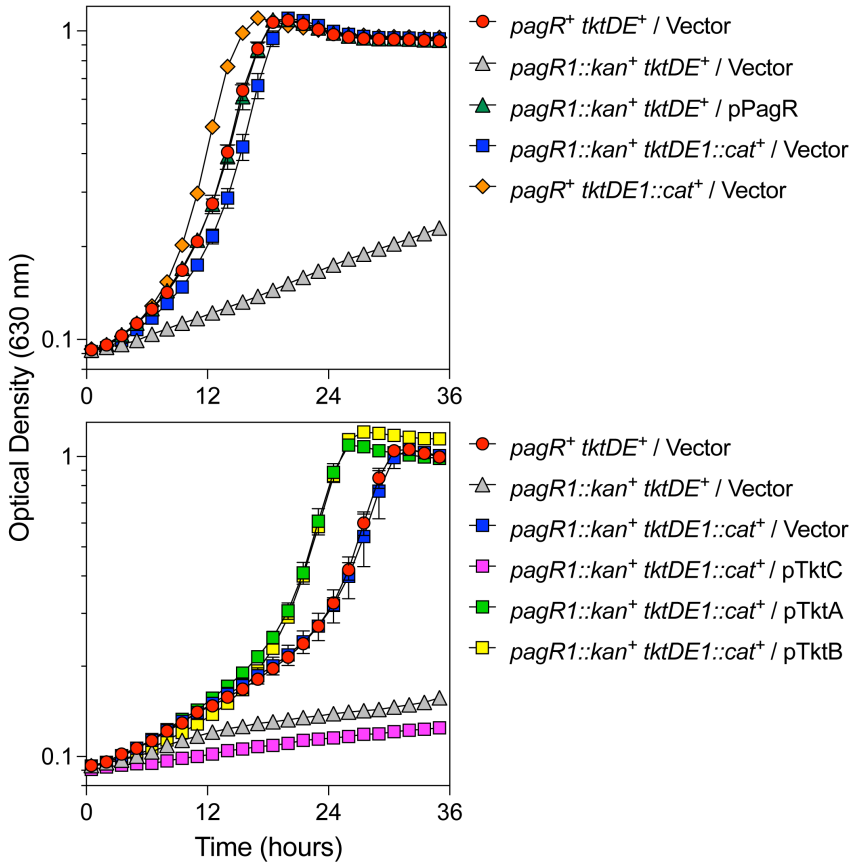


FIGURE 2 Growth of *Salmonella* Typhimurium on succinate as a function of *pagR* and *tktDE*. *Salmonella* Typhimurium was grown on NCE (no-carbon essential) minimal medium (Berkowitz et al., 1968) supplemented with sodium succinate (30 mM) as the sole source of carbon and energy. (a) The *pagR1*::*kan*$^+$ strain fails to grow after 36 h on succinate as the sole carbon source, and ectopic expression of *pagR*$^+$ restores growth to wild-type. Removal of *tktDE* in the *pagR1*::*kan*$^+$ background restores growth as well. Growth of the *pagR*$^+$ *tktDE*::*cat*$^+$ strain does not significantly differ from the parent strain. Ectopic gene expression was induced with 100 μM of L-(+)-arabinose. "pPagR" refers to pPagR-7. (b) Overproduction of TktC, but not TktA or TktB, represses growth of the *pagR1*::*kan*$^+$ *tktDE*::*cat*$^+$ strain. Ectopic gene expression was induced with 1 mM of L-(+)-arabinose. The strains used were *pagR*$^+$ *tktDE*$^+$/vector (JE22070, red circles), *pagR1*::*kan*$^+$ *tktDE*$^+$/vector (JE21566, gray triangles), *pagR1*::*kan*$^+$ *tktDE*$^+$/pPagR (JE21577, dark green triangles), *pagR*$^+$ *tktDE1*::*cat*$^+$/vector (JE25521, orange diamonds), *pagR1*::*kan*$^+$ *tktDE1*::*cat*$^+$/vector (JE25523, blue squares), *pagR1*::*kan*$^+$ *tktDE1*::*cat*$^+$/pTktC (JE25524, magenta squares), *pagR1*::*kan*$^+$ *tktDE1*::*cat*$^+$/pTktA (JE257201, light green squares), *pagR1*::*kan*$^+$ *tktDE1*::*cat*$^+$/pTktB (JE27202, yellow squares); 'vector' stands for the empty cloning vector pCV1 that contains an arabinose-inducible promoter (Vandrisse & Escalante-Semerena, 2016). This experiment was conducted in technical triplicate of biological duplicates three independent times. Error bars represent one standard deviation from the mean. Error bars that are not visible are smaller than the symbol.

plus ampicillin and 100 μM L-(+)-arabinose, then we quantified β-galactosidase activity following a described protocol (Miller & Hershberger, 1984). The β-galactosidase activity of the *pagR3*::*lacZY*$^+$ strain was significantly lower in the strain expressing *pagR* than in the vector control (Figure 3b, blue vs. red bars).

We also tested whether *tktDE* expression was altered in the *pagR1*::*kan*$^+$ strain grown in a low-phosphate, low-magnesium N-medium (LPM medium), since *pagR* is upregulated in this medium (Jiang et al., 2020). Cells were grown to OD_{600} of ~0.5 in LPM medium supplemented with L-(+)-arabinose (100 μM) and RNA was harvested. We observed that expression of *tktDE* was significantly higher in the *pagR1*::*kan*$^+$ strain, and the magnitude of the increase was higher than for cells grown in LB (Figure 3c, ~50× vs ~10×, respectively). This suggested that low phosphate and low magnesium activated expression of *tktDE* as well as *pagR*. Together, these data demonstrated that PagR repressed the expression of the cluster containing *tktDE*, and its own gene. This conclusion was consistent with its annotated homology to the LacI/GalR family of repressors.

2.3 | The *tktD and tktE* genes are part of a five-gene operon

Bioinformatics analysis suggested that genes *stm2340 (tktE)*, *stm2341 (tktD)*, *stm2342*, *stm2343*, and *stm2344* comprised a polycistronic operon (Biocyc.org). To test this possibility, we performed operon PCR with RNA isolated from a *pagR1*::*kan*$^+$ strain. This strain was chosen because we know that *tktDE* and *stm2343* are highly expressed in this background. The RNA was treated with DNase, and cDNA was generated from purified total RNA.

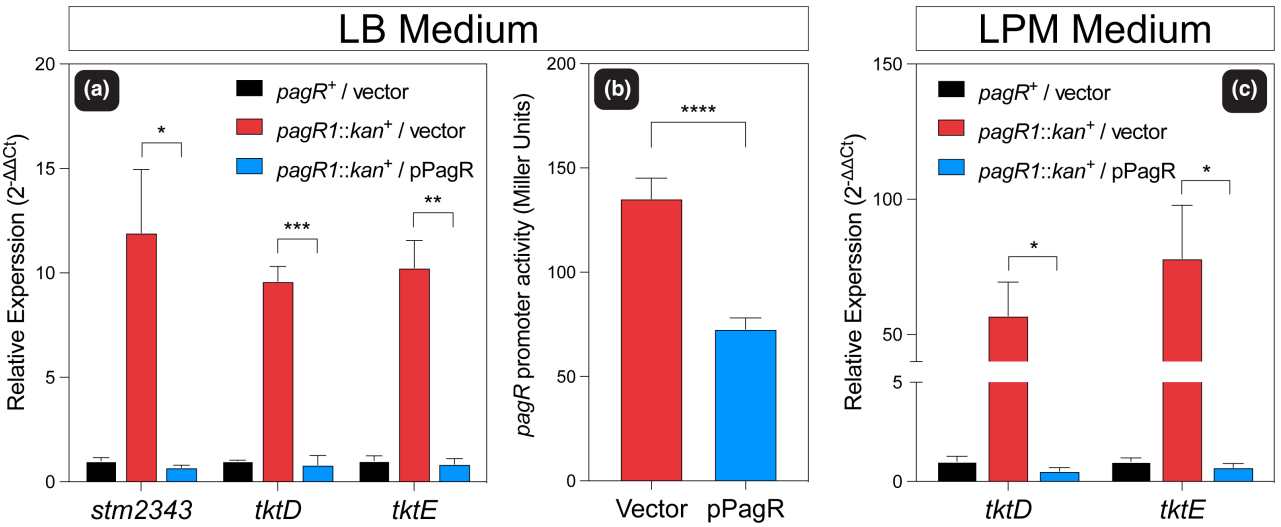


FIGURE 3 Expression analysis of the operon containing *tktDE* and of *pagR*, as a function of PagR. (a) Effect of PagR on the expression of *stm2343*, *tktD*, and *tktE* for cells grown in LB as shown by RT-qPCR. The experiment was performed in biological and technical triplicates. (b) Activity of the *pagR* promoter (in Miller Units) without and with $pagR^+$ expressed *in trans* (red vs. blue bars, respectively). (c) Effect of PagR on the expression of *tktD* and *tktE* for cells grown in LPM medium as shown by RT-qPCR $^*p \le 0.05$; $^{**}p < 0.01$; $^{***}p \le 0.001$; $^{****}p \le 0.0001$. Cultures were grown in LB, and details of the RT-qPCR and β-galactosidase assay conditions used can be found in Section 2. Vector = pCV1 (Vandrisse & Escalante-Semerena, 2016).

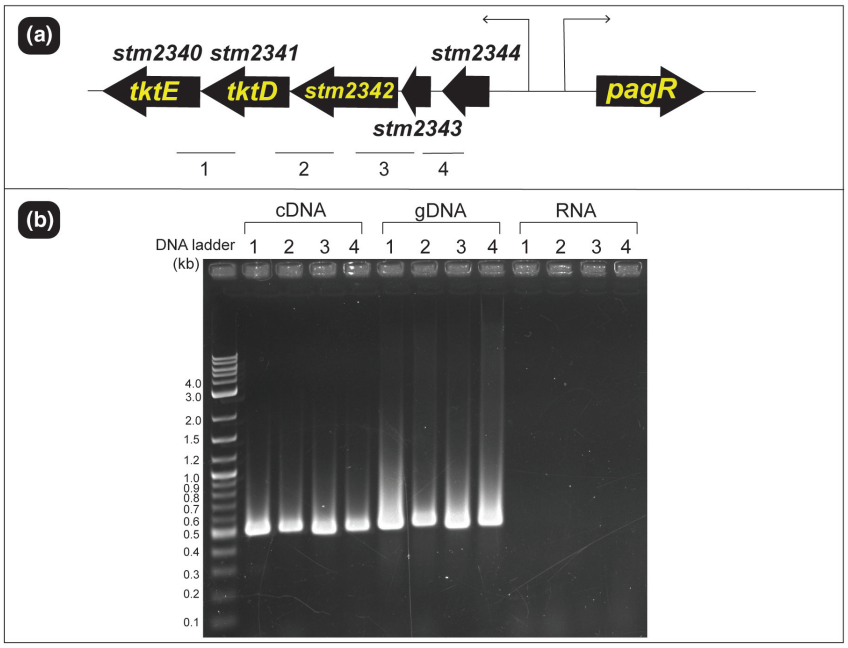


FIGURE 4 Genes encoding TktD and TktE are promoter-distal in a five-gene operon. (a) The *pagR* gene is divergently transcribed from the operon containing the genes encoding the two subunits of TktC (*tktD* and *tktE*). The first three genes of the operon are annotated as putative phosphotransferase system (PTS)-type transporters. (b) Operon PCR of the putative polycistronic operon containing the transketolase genes *tktD* and *tktE* encoding the subunits of TktC. RNA, cDNA, and gDNA were PCR amplified using primers specific to overlapping regions between genes of the putative operon designated 1–4 in panel (a). Positive controls are amplification of gDNA; negative controls are no amplification of RNA samples; experimental samples were the cDNA amplifications. Ladder on left shows corresponding amplification size (2-log DNA Ladder, NEB).

Genomic DNA, cDNA, and RNA were PCR amplified with four primer sets to generate products of four potential regions that overlap in neighboring putative genes (Figure 4a). As shown in Figure 4b, the use of such primers generated amplicons for the cDNA and the gDNA, but none amplified for the RNA, which served as the negative control. PCR amplification of all overlapping regions between genes *stm2340* and *stm2344* suggested these genes were part of a polycistronic unit.

2.4 | PagR binds directly to the intergenic region between *pagR* and the five-gene operon encoding *tktD and tktE*

To determine whether PagR directly bound to the promoter driving the expression of the *tktD and tktE* genes or was acting indirectly to repress the expression of the operon, PagR protein was purified to >95% homogeneity (Figure S2) and tested for its ability to bind to the putative promoter region between *stm2344* and *pagR*. The putative promoter fragment of *pagR* and the polycistronic operon comprised of the *stm2340-stm2344* genes was incubated with increasing concentrations of PagR protein then separated by native polyacrylamide electrophoresis (Figure 5). The mobility of the DNA fragment (2,457,048–2,457,454 nt of the chromosome; 406 nt) that included the putative promoter region decreased as a function of increasing concentrations of PagR protein as compared to the no-PagR-protein-added control. Collectively, these results suggested that the oligomerization state of PagR changed as its concentration increased or that multiple PagR-binding sites were present in the DNA fragment. Moreover, PagR did not affect the migration of a probe spanning the *acs* promoter (4,515,674–4,515,972 nt of the chromosome; Figure 5, right panel), indicating that the effect of PagR on the *stm2344–pagR* promoter was specific.

2.5 | PagR protects two binding sites in the *stm2344–pagR* Promoter region

DNase I footprinting was performed using a 291-nt DNA fragment spanning from 2,457,048 to 2,457,339 nt of the chromosome to define the DNA sequence bound by PagR. Results of an EMSA comparing PagR binding to this fragment with the one used in Figure 4 suggested that the shorter probe used here contains all the relevant PagR-binding sites (Figure S3). Figure 6 shows the digestion results for the coding strand of the operon containing *tktD* and *tktE* (left to right going toward *stm2344*). The presence of PagR (Figure 6, black trace) clearly protected two 21 base pair regions of the *stm2344–pagR* promoter region that were not protected without PagR (Figure 6, orange trace). A nearly identical sequence was observed in both (Figure 6, red underlines). The underlined sequence in the protected region on the left is a perfect 14 base pair palindrome, 5′-TGATAGCGCTATCA-3′, and the protected region on the right differs at only 2 bases (5′-TGGTAGCGCTATCT-3′, differences underlined). The protected regions were identified by aligning electropherogram traces (Figure S4a) with DNA1 digestion traces (Figure S4b). These data supported the conclusion that PagR was a LacI/GalR family regulator, since LacI/GalR family repressors typically bind palindromic or inverted repeat DNA (Weickert & Adhya, 1992).

2.6 | PagR is likely a member of the LacI/GalR family of transcriptional regulators

Herein, we have presented data showing that PagR is likely a member of the LacI/GalR regulator family, but a co-effector for PagR is yet to be identified. PagR represses its own expression, and the expression of adjacent genes encoding a putative transport system and subunits of a metabolic enzyme (Figure 5). Moreover, PagR binding to the promoter region between its gene and *stm2344* protects a palindromic DNA sequence (Figure 6). The repressor activity of PagR presented here contrasts with previous data reported by others, who showed that PagR is an activator of the *slyA* gene (Jiang et al., 2020). This dual activity, however, is not unheard of for LacI/GalR family proteins (Swint-Kruse & Matthews, 2009). It is currently unknown what causes the switch between these functions for PagR. It is possible that the target of the uncharacterized, putative phosphotransferase system (PTS) (*stm2342-4*) adjacent to *pagR* may provide the signal, like galactose derepressing GalR (Swint-Kruse & Matthews, 2009). Expression of *pagR* increases under low-phosphate and low-magnesium conditions (Jiang et al., 2020), and it could be that PagR is regulated by phosphorylation or as a function of magnesium ions.

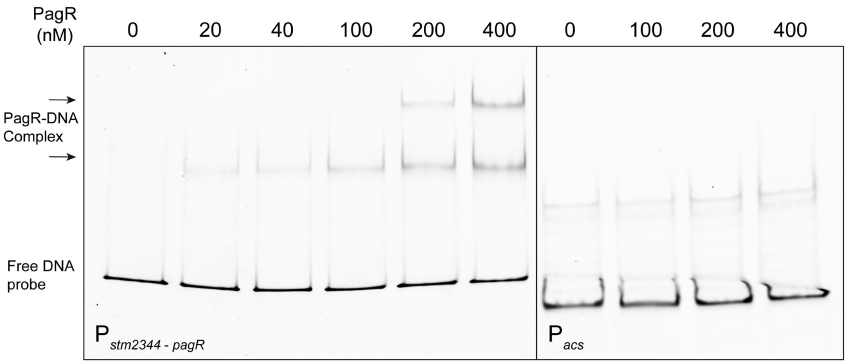


FIGURE 5 PagR binds the region between *pagR* and the five-gene operon that includes *tktD and tktE*. Representative results of an experiment designed to determine whether PagR could bind to the intergenic region between *pagR* and the five-gene operon containing genes encoding TktC. In this experiment we used 0.5 pmol of probe. The experiment was repeated three times and the amount of free probe (406 nt) decreased as a function of the amount of PagR added to the reaction mixture. More details about how the experiment was performed can be found under Section 2.

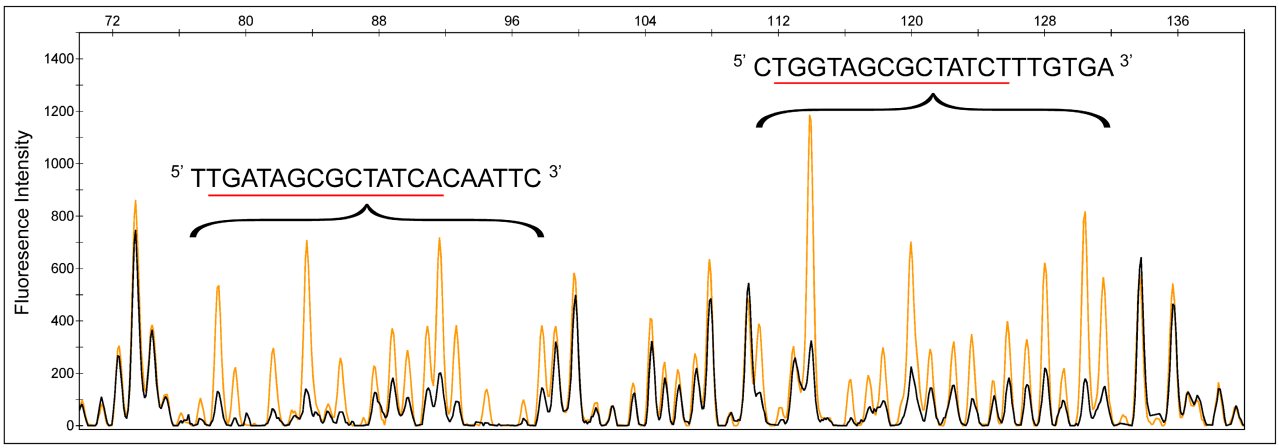


FIGURE 6 PagR binds two regions of the *stm2344* promoter. DNase 1 footprinting electropherograms from the coding strand of $P_{stm2344}$. Digestions were performed with 75 pmol PagR (black trace) and with no PagR (orange trace). This image is representative of two independent experiments.

2.7 | What is the connection between succinate catabolism and transketolase C?

That is an intriguing question that maybe best addressed within the framework of a *S*. Typhimurium infection. Recent work by others has shown that succinate accumulates in macrophages during a *S*. Typhimurium infection and that the transport of this TCA cycle intermediate is required for survival of this bacterium within macrophages (Rosenberg et al., 2021). These authors proposed that *S*. Typhimurium uses succinate within the macrophage to trigger its virulence and survival mechanisms. How TktC and the other functions encoded by the operon fit within that framework remains to be determined.

3 | CONCLUSIONS

Previous work demonstrated that PagR is necessary for full induction of the SPI-2 type-3 secretion system (Jiang et al., 2020). Our data show that PagR also regulates expression of the genes encoding the subunits of the TktC transketolase (i.e., *tktD*, *tktE*), the third transketolase enzyme identified in *S*. Typhimurium (Shaw et al., 2018). We also identified the binding sites for PagR in the region between *stm2344* and *pagR*. The perfect palindrome identified in this study (5′-TGATAGCGCTATCA-3′) is similar to a sequence in the *slyA* promoter probe used by Jiang et al. (5′-TGTAAGGGCAATCC-3′, differences underlined). While this sequence has not been shown to be the PagR-binding site in the *slyA* promoter, its presence suggests that the sequences we identified may be helpful in finding other targets of PagR.

Transketolases are essential for *S*. Typhimurium virulence (Shaw et al., 2018), and PagR appears to be a link between genetic regulation of the pathogenic machinery and a metabolic function essential for the pathogenic lifestyle of this bacterium. Moreover, the data presented here suggest that TktC may have a function in the cell different than that of TktA and TktB. Future research into the signal to switch from repression to activation for PagR, and into the function of TktC, will illuminate the connections between central metabolism and the pathogenic machinery in *S*. Typhimurium.

4 | EXPERIMENTAL PROCEDURES

4.1 | Bacterial strains

All strains were derivatives of *Salmonella enterica* subsp. *enterica* serovar Typhimurium str. LT2 (hereafter *S*. Typhimurium; Table 1). Gene deletions were constructed using the protocol that employs λ Red recombinase to engineer in-frame deletions as described elsewhere (Datsenko & Wanner, 2000).

4.2 | Deletion strain construction

Primers used in this study were synthesized by Integrated DNA Technologies, Inc. (IDT), and are listed in Table 2. The *pagR1*::*kan*$^+$ and *tktDE1*::*cat*$^+$ markers were engineered as follows: PFU Ultra II Fusion DNA polymerase (Stratagene) was used to amplify flanking regions of plasmids pKD3 (*cat*$^+$ marker) or pKD4 (*kan*$^+$ marker) using primers designed with 36 bp of overlapping region to the beginning or the end of *pagR* or *tktD-tktE* genes. Polymerase chain reaction (PCR) amplicons were visualized by poststaining with ethidium bromide (0.5 mg/mL) for 10 min. Products were cleaned with the Wizard® SV gel and PCR clean up kit (Promega), and ~200 ng of PCR product was electroporated into *S*. Typhimurium strain JE6692 (*metE205* Δ*araB9*/pKD46 *bla*$^+$) using a 0.2-cm electroporation cuvette (MidiSci) and a microPulser electroporator (Bio-Rad Laboratories) on Ec2 setting. Cells were recovered by incubation at 37°C with

TABLE 1 Strains and plasmids used in this study.

Strain	Relevant genotype	Reference/source
S. Typhimurium[a] strains		
JE6583	*metE205 ΔaraB9*	K. Sanderson via J. Roth
Derivatives of JE6583		
JE22070	/pCV1 (cloning vector) *bla*$^+$	VanDrisse and Escalante-Semerena (2016)
JE21107	*pagR1*::*kan*$^+$	
JE24887	*ΔpagR2* resolved	
JE27072	*pagR3*::*lacZY*$^+$ *kan*$^+$	
JE25373	*tktDE1*::*cat*$^+$	
JE25443	*pagR1*::*kan*$^+$ Δ*tktDE1*::*cat*$^+$	
JE21566	*pagR1*::*kan*$^+$/pCV1 *bla*$^+$	
JE21577	*pagR1*::*kan*$^+$/pPagR-7 *bla*$^+$	
JE25521	*pagR*$^+$ *tktDE*::*cat*$^+$/pCV1 *bla*$^+$	
JE25523	*pagR1*::*kan*$^+$ *tktDE1*::*cat*$^+$/pCV1 *bla*$^+$	
JE25524	*pagR1*::*kan*$^+$ *tktDE1*::*cat*$^{+/}$pTktC-1 *bla*$^+$	
JE27201	*pagR1*::*kan*$^+$ *tktDE1*::*cat*$^{+/}$ pTktA-1 *bla*$^+$	
JE27202	*pagR1*::*kan*$^+$ *tktDE1*::*cat*$^{+/}$ pTktB-1 *bla*$^+$	
JE27091	*pagR3*::*lacZY*$^+$ *kan*$^+$/pCV1 *bla*$^+$	
JE27092	*pagR3*::*lacZY*$^+$ *kan*$^+$/pPagR-7 *bla*$^+$	
JE6692	/pKD46 *bla*$^+$	Laboratory collection
E. coli strains		
E. coli C41 (λDE3)	*pka12*::*kan*$^+$ *ompT hsdS* (r_Bm_B) *gal* (λDE3)	Laboratory collection
E. coli DH5α	Δ(*argF-lacZ)169 ΔphoA8 l*$^-$f80d*lacZ58*(M15) *thiE1 glnX44*(AS) *deoR481 hsdR17 gyrA96*(Nal^R) *recA1 endA1*	Laboratory collection

[a]*S.* Typhimurium = *Salmonella enterica* subsp. *enterica* sv. Typhimurium strain LT2.

shaking and plated on LB (Difco) agar supplemented with either 12.5 μg/mL of chloramphenicol for the *cat*$^+$ marker or 25 μg/mL of kanamycin for the *kan*$^+$ marker. Correct antibiotic insertions were PCR verified then moved by P22-mediated transduction into strain JE6583 as described elsewhere (Davis et al., 1980). Colonies were streaked to isolation and the genomes of isolated colonies were sequenced using Sanger sequencing technology to verify correct insertion location and sequence using primers flanking genes of interest.

4.3 | Construction of *pagR3*::*lacZY* chromosomal fusion strain

The kanamycin resistance cassette was resolved from strain JE21107 (*pagR1*::*kan*$^+$, yielding Δ*pagR2*) using pCP20 and a method described elsewhere (Datsenko & Wanner, 2000). The *lacZY*$^+$ fusion was created by FLP-mediated integration of pKG136 (Ellermeier et al., 2002). Briefly, pCP20 was transformed into the resolved Δ*pagR* strain (JE24887). Plasmid pKG136 was transformed into the resulting strain and cells were recovered overnight in LB at 37°C. The next morning cells were plated on LB agar with 50 μg/mL kanamycin to select for integration. Correct *lacZY*$^+$ *kan*$^+$ insertions were PCR verified then moved by P22-mediated transduction into strain JE6583 (Davis et al., 1980).

4.4 | Plasmid construction for complementation of function and gene overexpression

All plasmids used here are listed in Table 3.

The high-efficiency cloning method of BspQI digestion described elsewhere (Galloway et al., 2013; VanDrisse & Escalante-Semerena, 2016) was used to clone *pagR* into plasmids pCV1 and pTEV19, and *tktD-tktE*, *tktA*, and *tktB* into pCV1. All genes cloned were PCR amplified from *S.* Typhimurium strain JE6583 genomic DNA using PFU Ultra II Fusion DNA polymerase and PCR products were visualized as described above. PCR products were cleaned using the Promega Wizard® SV gel and PCR clean up kit, and cloning using the method cited above. After transformation into *Escherichia coli* DH5α cells and colony PCR screening of correctly ligated plasmids, plasmids were isolated using the Wizard®

TABLE 2 Primers and DNA probes used in this study.[a]

Primer name	Primer sequence 5′→3′
EMSA primers	
5′_*pagR*_EMSA (5′ 6-FAM label)	CGCAAATTTCCAGCGCCTGCG
3′_*pagR*_EMSA (5′ HEX label)	TACACCGGCAAGTTGGGCTAC
5′_*acs*_EMSA (5′ 6-FAM label)	ATGTGTTTGGCTCATGCTGT
3′_*acs*_EMSA	AGTGTATGTAAAATACCACTTTAGAG
Deletion, Cloning, and RT-qPCR primers	
5′_*pagR*_wanner	ATGTCGATACCCCGTAAACG GCGCAGTA CCGGTAAAGTGTAGGCTGGA GCTGCTTC
3′_*pagR*_wanner	TTAGCAGCTTTCCCGCATAC ATAAACTG GAGGCGATCATATGAATATC CTCCTTAG
5′_*pagR*_BspQI	NNGCTCTTCNTTCATGTCGATACCCC GTAAACG
3′_*pagR*_BspQI	NNGCTCTTCNTTATTAGCAGCTTTCC CGCATAC
5′_*tktD*_BspQI	NNGCTCTTCNTTCATGAACGTAA CCGAAA
3′_*tktE*_BspQI	NNGCTCTTCNTTATTAAAGCAGT GATTTCG
5′_*tktA*_BspQI	NNGCTCTTCNTTCATGTCCTCACGTA AAGAGCTTG
3′_*tktA*_BspQI	NNGCTCTTCNTTATTACAGCAGTGCT TTCGCTT
5′_*tktB*_BspQI	NNGCTCTTCNTTCATGTCCCGTA AAGACCTTGC
3′_*tktB*_BspQI	NNGCTCTTCNTTATTAGCCTTTGATG TTTAGCACC
5′_*tktD*_wanner	TCACCCAACTGGCGCGCGAT ATTCGCGT CGCCACGCGTGTAGGCTGGA GCTGCTTC
3′_*tktE*_wanner	TTTCGCGGCTTCTACAATCGCTT CGGCGG TGAGTCCCATATGAATATCCTCCTTAG
5′_*stm2343*_qPCR	GTTCCGGCCTGGGTAGTAGTT
3′_*stm2343*_qPCR	CCGATGAAAGATCGGAGTGT
5′_*tktD*_qPCR	CGATGATATCGCCGGACTAC
3′_*tktD*_qPCR	CCTCATTGAGCGTCTGCTTC
5′_*tktE*_qPCR	CTATCGATCGCATGTTGGTG
3′_*tktE*_qPCR	CTGCCCATAACGCTCTTTGA
Operon PCR primers	
5′_operon PCR_1	AGCGCCATAAAGAGCTGA
3′_operon PCR_1	CGATGATATCGCCGGACTAC
5′_operon PCR_2	TATTCAGCTCTTCGCGCG
3′_operon PCR_2	TCCTGCCAGTGCTGTTAC
5′_operon PCR_3	ACATACCCCCTAGCGG
3′_operon PCR_3	GTTCCGGCCTGGGTAGTAGTT
5′_operon PCR_4	CCGATGAAAGATCGGAGTGT
3′_operon PCR_4	TTGGGCCATATTATGTATTAGCG
DNase 1 footprinting primers	
5′_sequencing template	GGTACTGCGCCGTTTAC
3′_sequencing template	GAACAATCGCCGTAAGGTATTC
5′_digestion/sequencing (5′ 6-FAM label)	CGCAAATTTCCAGCGCCTGCG (same as 5′_*pagR*_EMSA)
3′_digestion/sequencing (5′ HEX label)	TGTCGTTCTTTGCTTCGCATGAC

[a]All primers were manufactured by Integrated DNA Technologies (IDT, Coralville, IA, USA).

Plus SV miniprep kit (Promega). Sanger DNA sequencing was performed by Eton Bioscience to rule out mutations and confirm insertions.

4.5 | Culture media, chemicals, and in vivo growth analyses

Growth behavior studies were conducted as follows: (i) starter bacterial cultures were grown from a single colony in nutrient broth (NB, Difco) with overnight shaking at 180 rpm at 37°C; (ii) after ~16 h of growth, cells (~10^8 cfu) were subcultured into no-carbon essential (NCE) minimal medium (Berkowitz et al., 1968) containing $MgSO_4$ (1 mM), Wolfe's trace minerals (Balch & Wolfe, 1976), ampicillin (100 μg/mL), L-(+)-arabinose (concentration stated in figure legends), with sodium succinate (30 mM) as the sole carbon and energy source. Inoculum used was routinely 1% (v/v) of the final volume of the culture. Growth studies were performed in 96-well polystyrene (Falcon) microtiter plates with each well containing 198 μL of fresh medium and a 2-μL inoculum. Microtiter plates were incubated at 37°C shaking continuously inside a PowerWave microtiter plate reader (Bio-Tek Instruments). Density of cells was monitored at 630 nm and data were analyzed using Prism 9 (GraphPad).

4.6 | Alignment and visualization of PagR amino acid sequence with LacI/GalR family members

Amino acid sequences were obtained from Biocyc.org for the following proteins from *S.* Typhimurium: PagR (STM2345), GalR, and CytR, and the following from *E. coli* K-12 substr. MG1655 (*E. coli*): LacI, GalR, and CytR. The sequences were aligned using Clustal Omega with default settings. The alignment was visualized using ESPript 3.0 with default settings and Flashy color scheme (Robert

TABLE 3 Plasmids used in this study.

Plasmid	Genotype	Description	Reference/source
pCV1	*araC*$^+$ *bla*$^+$	P_{araBAD} expression vector	Vandrisse and Escalante-Semerena (2016)
pTEV19	*bla*$^+$	Overexpression vector for MBP-H_6-*N*-terminally tagged rTEV-cleavable protease	Vandrisse and Escalante-Semerena (2016)
pPagR-7	*pagR*$^+$ *bla*$^+$	*pagR*$^+$ (*stm2345*$^+$) cloned into pCV1	
pTktC-1	*tktD*$^+$ *tktE*$^+$ *bla*$^+$	*tktD*$^+$ and *tktE*$^+$ cloned into pCV1	
pTktA-1	*tktA*$^+$ *bla*$^+$	*tktA*$^+$ cloned into pCV1	
pTktB-1	*tktB*$^+$ *bla*$^+$	*tktB*$^+$ cloned into pCV1	
pPagR-8	*pagR*$^+$ *bla*$^+$	*pagR* $^+$ (*stm2345*$^+$) cloned into pTEV19	
pCP20	*flp*$^+$ *bla*$^+$ *cat*$^+$	FLP expression plasmid, temperature sensitive above 37°C	Cherepanov and Wackernagel (1995)
pKG136	*lacZY*$^+$ *kan*$^+$	For FLP integration of *lacZY*$^+$ *kan*$^+$ cassette at FLP-resolved deletion sites	J.M. Slauch

& Gouet, 2014). Secondary structure data from *E. coli* LacI was imported to ESPript from Protein Data Bank entry 4RZS.

4.7 | RNA isolation

Strains JE22070 (*pagR*$^+$/vector), JE21566 (*pagR1*::*kan*$^+$/vector), and JE21577 (*pagR1*::*kan*$^+$/pPagR) were grown overnight in triplicate in nutrient broth (2 mL; NB, Difco) with shaking at 37°C. After incubation, cultures were diluted 1:100 into 5 mL of fresh LB-rich medium supplemented with L-(+)-arabinose (100 μM) or 5 mL low-phosphate, low-magnesium N-medium (Jiang et al., 2020) supplemented with L-(+)-arabinose (100 μM). Cultures were grown shaking at 37°C to an optical density of 0.5 at 600 nm, then 5 mL of each sample were quickly centrifuged in 15-mL Falcon tubes at 4000*g*, supernatant was removed, and pellets were flash-frozen in liquid nitrogen and kept on dry ice. RNA was isolated following the RNAsnap™ protocol (Stead et al., 2012). Pellets were resuspended in 150 μL of boil solution (ethylenediaminetetraacetic acid (EDTA, 18 mM), SDS (0.025%, w/v) formamide (95%, v/v; RNA grade), 2-mercaptoethanol (1% v/v) in RNase-free water) and were vortexed vigorously to break up the cell pellet. Pellets were incubated at 95°C for 7 min and centrifuged at 16,000*g* for 5 min at room temperature; 100 μL of supernatant was transferred to a fresh tube. A sodium acetate/ethanol RNA precipitation was then conducted by the addition of 400 μL of RNase-free water, 50 μL of sodium acetate (3 M, pH 5.2: final concentration of 0.3 M), and finally 1.65 mL of ice-cold absolute ethanol (100%), with mixing briefly before the addition of the next reagent. The mixture was incubated at −80°C for 1 h, centrifuged at 16,000*g* for 30 min at 4°C, and ethanol was decanted. Ethanol (300 μL of cold 70% v/v) was added, and pellets were centrifuged at 8000*g* for 5 min at 4°C in an Eppendorf 5415D centrifuge. Ethanol was removed and pellets were allowed to dry. RNA pellets were resuspended in RNase-free water. Subsequent RNase-free DNase I treatment was conducted using the Ambion Turbo DNA-free kit according to manufacturer's instructions (ThermoFisher Scientific). After DNA cleavage, a final sodium acetate/ethanol precipitation was performed as described above, except using 360 μL of water, 50 μL of 3 M sodium acetate, and 1.5 mL of cold 100% ethanol. After overnight incubation at −80°C, RNA was centrifuged at 16,000*g* for 30 min, then washed with 300 μL of cold 70% ethanol (v/v). Ethanol was decanted, and RNA pellets were dried for 20 min at room temperature. RNA was resuspended in 100 μL of water. A small sample of each preparation was used for quantification with the RNA Broad Range (BR) Assay kit by Qubit on a Qubit 4 fluorometer. A small amount of each preparation was also tested for quality and integrity using the Qubit RNA IQ Assay. Primers for qPCR were designed using Primer3 (Koressaar et al., 2018; Koressaar & Remm, 2007; Untergasser et al., 2012).

4.8 | cDNA synthesis and real-time quantitative polymerase chain reaction

Total RNA from each sample was used for the synthesis of cDNA using the iScript™ cDNA synthesis Kit from Bio-Rad Laboratories according to manufacturer's protocol. Each cDNA reaction was then diluted to 7.5 ng/μL and used as template for PCR. For real-time PCR, 20 μL reactions were prepared with 10 μL of 2X FastSYBR Green master mix (Applied Biosystems), 500 nM of each gene-specific primer (1 μL of 10 μM primer stock), and 15 ng of cDNA (2 μL of 7.5 ng/μL cDNA). The real-time PCR reaction was performed using a 7500 Fast real-time PCR system (Applied

Biosystems). The threshold cycle value of *gyrB* were checked first to ensure it was optimal for use as reference genes for these strains under the conditions chosen for RT-qPCR. Cycle threshold (C_T) data were normalized to the *gyrB* gene. These normalized values (ΔC_T) were transformed using the $2(e\text{-}\Delta C_T)/10^{-6}$ method (Livak & Schmittgen, 2001), and were reported as the gene expression ratio ($2\text{^}\Delta\Delta C_T$) of the mutant strains/the parent strain (JE22070 *pagR*$^+$). Mean $2\text{^}\Delta\Delta C_T$ values were used to calculate the standard error of the mean (SEM) using Prism9 (GraphPad) from three biological replicates that were each tested in technical triplicate. Differences in $2\text{^}\Delta\Delta C_T$ between strains were compared using Welch's *t*-test with Prism9 software.

4.9 | β-Galactosidase assays

Plasmids pCV1 and pPagR-7 were independently transformed into JE27072 (*pagR*::*lacZY*$^+$ *kan*$^+$). Three independent colonies of each strain were grown overnight in 2 mL of NB plus ampicillin (100 μg/mL), then subcultured 1:100 into 5 mL of LB plus ampicillin (100 μg/mL) and arabinose (100 μM). Cells were grown shaking at 180 rpm at 37C until an OD_{600} nm of 0.4–0.6, and β-galactosidase units were measured as described (Miller & Hershberger, 1984).

4.10 | Operon PCR

As described above, total RNA was isolated from strain JE21107 (*pagR1*::*kan*$^+$) and was used to generate cDNA. cDNA and genomic DNA isolated from strain JE21107 were used in PCR reactions containing Green GoTaq (Promega) master mix to amplify overlapping genes within the *stm2340-stm2344* operon. Primer pairs are listed in Table 2.

4.11 | Purification of PagR protein

PagR protein was purified to homogeneity from plasmid pPagR-8 encoding a PagR protein with a maltose-binding protein-hexahistidine (MBP-H6) tag fused to its N terminus. The tag was removed after incubation with recombinant tobacco etch virus (rTEV) protease since the plasmid used to produce MBP-H_6-PagR (pTEV19) contained an rTEV protease cleavage site (VanDrisse & Escalante-Semerena, 2016). A sample (10 mL) of an overnight culture of *E. coli* C41 (λDE3)/pPagR-8 strain was used to inoculate 1 L of LB containing 100 μg/mL of ampicillin. Cells were grown shaking at 125 rpm at 37°C until the culture reached an optical density at 600 nm of 0.7. Expression of genes of interest encoded by the plasmids was induced by the addition of isopropyl β-D-1-thiogalactopyranoside (IPTG, 0.25 mM) followed by ~12 h of overnight incubation at 37°C. The next morning cells were harvested by centrifugation at 6000*g* for 15 min using a refrigerated Beckman-Coulter Avanti J-20-XPI centrifuge equipped with a JLA 8.1 rotor. Cell pellets were resuspended in 20 mL of buffer A [(4-(2-hydroxyethyl-1-piperazineethanesulfonic acid (HEPES) buffer (50 mM, pH 7.5 at 4°C) containing NaCl (0.5 M), glycerol (20% v/v), and imidazole (20 mM)] and were sonicated thrice for 30-s intervals, and during each interval, sonication was on for 2 s and off for 2 s, at 60% amplitude. The resulting whole-cell lysates were centrifuged for 30 min at 40,000*g* and the supernatants were filtered with a 0.45-μm filter (VWR) to remove large particulates. Each filtered lysate was applied onto a 1-mL nitrilotriacetic acid (NTA) affinity chromatography column pre-equilibrated with buffer A. Fractions were collected by gravity at 4°C. The purification was performed as follows: After all the lysate was loaded onto the column, the column was washed with 10 column volumes (CV, i.e., 10 mL) of buffer A, seven CV (i.e., 7 mL) of buffer A containing 4% elution buffer B [HEPES buffer (50 mM, pH 7.5 at 4°C), NaCl (0.5 M), glycerol (20% v/v), and imidazole (0.5 M)], and finally, MBP-H_6-PagR was eluted in two fractions, first with one CV (i.e., 1 mL) of 100% elution buffer B, and the second fraction being four CV (i.e., 4 mL) of 100% elution buffer B. Both elution fractions were pooled and MBP-H_6-PagR was cleaved with rTEV protease at a 1 mg 1:100 rTEV:PagR protein ratio while dialyzing at room temperature in HEPES buffer (50 mM, pH 7.5 at 4°C) containing NaCl (0.5 M), glycerol (10% v/v), and dithiothreitol (DTT, 1 mM). Cleaved protein was dialyzed twice more at 4°C in buffer A. Cleaved PagR protein was loaded again onto a 2-mL NTA column to remove MBP-His and rTEV protease, both of which were fused to a hexahistidine tag. Tag-less PagR protein did not interact with the NTA resin and was collected in the flow-through fraction. To further remove MBP from PagR, flow-through fractions from the second NTA purification were run over a 1-mL amylose resin to remove contaminating MBP. Pure, tag-less PagR protein was dialyzed overnight against HEPES buffer (50 mM, pH 7.5 at 4°C) containing NaCl (150 mM) and glycerol (20% v/v) at 4°C. Fifteen mL of dialyzed PagR solution was dispensed into Eppendorf microcentrifuge tubes, flash frozen in liquid nitrogen and stored at −80°C until used. Protein concentration was determined using the Qubit™ Protein Assay Kit (ThermoFisher) and the Qubit™ 4 fluorometer.

4.12 | Electrophoretic mobility shift assays

EMSAs were performed to quantify PagR binding to DNA. EMSAs were performed as follows: purified PagR protein was incubated at 0, 0.5, 1.0, 2.5, 5.0, and 10.0 pmol of protein with 0.5 pmol of a 5(6)-carboxyfluorescein (5(6)-FAM) and hexachlorofluorescein (HEX)-labeled DNA probe (1: from 2,457,048 to 2,457,454 nt of the chromosome; 406 nt, 2: from 2,457,048 to 2,457,339 nt of the chromosome; 291 nt). EMSA buffer [HEPES buffer (50 mM, pH 7.5 at 4°C) containing NaCl (150 mM), and glycerol (10% v/v)] was added to the reaction mixture (total volume = 25 μL) and DNA and protein were incubated at room temperature for 40 min. During incubation, a 7.5% Tris-Boric acid-EDTA (TBE) polyacrylamide gel was predeveloped at 100 V for 40 min in 0.5× TBE buffer at 4°C. After incubation, 5 μL of glycerol (50% v/v) was added to the reaction mixtures, and 20 μL of each reaction mixture was resolved by

the polyacrylamide gel. A lane of xylene cyanol and bromophenol blue dye was added as a tracking indicator, and the gel was run until bromophenol blue reached the bottom of the gel. The gel was imaged using a Typhoon Trio Imager (GE Healthcare) at 525 nm with the 488 (Blue) filter.

4.13 | DNase I footprinting

The promoter region of *stm2344* and *pagR* (from 2,457,048 to 2,457,339 nt of the chromosome; 291 nt) was PCR amplified using a 5(6)-FAM-labeled primer and a HEX-labeled primer from JE6583 genomic DNA. The product was purified with the Wizard® SV Gel and PCR Cleanup System (Promega). 7.5 pmol of 5(6)-FAM/HEX-labeled probe was incubated with either no PagR protein or 75 pmol PagR for 40 min at room temperature in 250 µL EMSA Buffer. Twenty-five ng of DNase I (Sigma) was added to each reaction and incubated for 5 min at room temperature. DNase was heat inactivated at 80°C for 10 min. Digested fragments were purified with the Wizard® SV Gel and PCR Cleanup System (Promega), eluted from the column with 30 µL diH_2O, and diluted 1:2 in diH_2O for analysis. Fragment analysis by capillary electrophoresis was performed at the University of Illinois DNA Core Sequencing facility using the Applied Biosystems 3730xl DNA Analyzer. The results were processed with GeneMapper6 and aligned to the sequencing results to determine the protected region(s) (Figure S4a,b).

4.14 | Dideoxy sanger sequencing

The promoter region of *stm2344/pagR* (from 2,456,991–2,457,412 nt of the chromosome; 421 nt) was PCR amplified from JE6583 genomic DNA and purified with the Wizard® SV Gel and PCR Cleanup System (Promega) to create a template for dideoxy termination sequencing. This template was sequenced using the USB® ThermoSequenase Cycle Sequencing Kit (Affeymetrix) with the HEX and 5(6)-FAM labeled primers used to generate the digested fragment. Sequencing was performed following the manufacturer's instructions for dideoxy termination sequencing using 2 pmol of primer, 200 ng template, and 60 cycles for each reaction. Samples were diluted 1:2 in deionized water and analyzed at the University of Illinois DNA Core Sequencing facility using the Applied Biosystems 3730xl DNA Analyzer. The resulting electropherograms were analyzed with GeneMapper™ Software 6 (Thermo Fisher Scientific).

AUTHOR CONTRIBUTIONS

Jorge C Escalante-Semerena: Conceptualization; formal analysis; supervision; visualization; funding acquisition; project administration. **Anastacia R. Parks:** Conceptualization; investigation; validation; methodology; formal analysis; data curation; writing – original draft. **Regan D. McCormick:** Conceptualization; methodology; investigation; validation; formal analysis; data curation. **Jordan A. Byrne:** Investigation.

ACKNOWLEDGMENTS

This work was supported by NIH grant R35-GM130399 to J.C.E.-S. The authors thank the DNA Services Lab of the Roy J. Carver Biotechnology Center of The University of Illinois at Urbana-Champaign for the performance of the DNAse I Footprinting Analysis.

CONFLICT OF INTEREST STATEMENT

The authors have no conflict of interest to declare.

DATA AVAILABILITY STATEMENT

All the data generated by these studies is reported in this paper and its Supplementary Information file.

ETHICS STATEMENT

No humans or animals were used in these studies.

ORCID

Anastacia R. Parks https://orcid.org/0000-0003-0425-0106
Regan D. McCormick https://orcid.org/0000-0001-6342-0051
Jordan A. Byrne https://orcid.org/0000-0002-9480-6587
Jorge C. Escalante-Semerena https://orcid.org/0000-0001-7428-2811

REFERENCES

Balch, W.E. & Wolfe, R.S. (1976) New approach to the cultivation of methanogenic bacteria: 2-mercaptoethanesulfonic acid (HS-CoM)-dependent growth of *Methanobacterium ruminantium* in a pressurized atmosphere. *Applied and Environmental Microbiology*, *32*, 781–791.

Berkowitz, D., Hushon, J.M., Whitfield, H.J., Jr., Roth, J. & Ames, B.N. (1968) Procedure for identifying nonsense mutations. *Journal of Bacteriology*, *96*, 215–220.

Cherepanov, P.P. & Wackernagel, W. (1995) Gene disruption in *Escherichia coli*: Tc^R and Km^R cassettes with the option of Flp-catalyzed excision of the antibiotic-resistance determinant. *Gene*, *158*(1), 9–14.

Datsenko, K.A. & Wanner, B.L. (2000) One-step inactivation of chromosomal genes in *Escherichia coli* K-12 using Pcr products. *Proceedings of the National Academy of Sciences of the United States of America*, *97*, 6640–6645.

Davis, R.W., Botstein, D. & Roth, J.R. (1980) *A manual for genetic engineering: advanced bacterial genetics*. Cold Spring Harbor, NY: Cold Spring Harbor Laboratory Press, pp. 78–79.

Ellermeier, C.D., Janakiraman, A. & Slauch, J.M. (2002) Construction of targeted single copy lac fusions using lambda red and FLP-mediated site-specific recombination in bacteria. *Gene*, *290*, 153–161.

Galloway, N.R., Toutkoushian, H., Nune, M., Bose, N. & Momany, C. (2013) Rapid cloning for protein crystallography using type IIS restriction enzymes. *Crystal Growth & Design*, *13*, 2833–2839.

Jiang, L., Wang, P., Li, X., Lv, R., Wang, L., Yang, B. et al. (2020) PagR mediates the precise regulation of *salmonella* pathogenicity Island 2 gene expression in response to magnesium and phosphate signals in *Salmonella* typhimurium. *Cellular Microbiology*, *22*, e13125.

Koressaar, T., Lepamets, M., Kaplinski, L., Raime, K., Andreson, R. & Remm, M. (2018) Primer3_masker: integrating masking of template sequence with primer design software. *Bioinformatics*, *34*, 1937–1938.

Koressaar, T. & Remm, M. (2007) Enhancements and modifications of primer design program Primer3. *Bioinformatics*, *23*, 1289–1291.

Livak, K.J. & Schmittgen, T.D. (2001) Analysis of relative gene expression data using real-time quantitative PCR and the 2(-ΔΔC(T)) method. *Methods*, *25*, 402–408.

Miller, F.D. & Hershberger, C.L. (1984) A quantitative beta-galactosidase alpha-complementation assay for fusion proteins containing human insulin B-chain peptides. *Gene*, *29*, 247–250.

Raines, C.A. (2003) The Calvin cycle revisited. *Photosynthesis Research*, *75*, 1–10.

Robert, X. & Gouet, P. (2014) Deciphering key features in protein structures with the new Endscript server. *Nucleic Acids Research*, *42*, W320–W324.

Rosenberg, G., Yehezkel, D., Hoffman, D., Mattioli, C.C., Fremder, M., Ben-Arosh, H. et al. (2021) Host succinate is an activation signal for *Salmonella* virulence during intracellular infection. *Science*, *371*, 400–405.

Schneider, G. & Lindqvist, Y. (1998) Crystallography and mutagenesis of transketolase: mechanistic implications for enzymatic thiamin catalysis. *Biochimica et Biophysica Acta*, *1385*, 387–398.

Shaw, J.A., Henard, C.A., Liu, L., Dieckman, L.M., Vazquez-Torres, A. & Bourret, T.J. (2018) *Salmonella enterica* serovar typhimurium has three transketolase enzymes contributing to the pentose phosphate pathway. *The Journal of Biological Chemistry*, *293*, 11271–11282.

Stead, M.B., Agrawal, A., Bowden, K.E., Nasir, R., Mohanty, B.K., Meagher, R.B. et al. (2012) Rnasnap: a rapid, quantitative and inexpensive, method for isolating total Rna from bacteria. *Nucleic Acids Research*, *40*, e156.

Stincone, A., Prigione, A., Cramer, T., Wamelink, M.M., Campbell, K., Cheung, E. et al. (2015) The return of metabolism: biochemistry and physiology of the pentose phosphate pathway. *Biological Reviews of the Cambridge Philosophical Society*, *90*, 927–963.

Swint-Kruse, L. & Matthews, K.S. (2009) Allostery in the LacI/GalR family: variations on a theme. *Current Opinion in Microbiology*, *12*, 129–137.

Untergasser, A., Cutcutache, I., Koressaar, T., Ye, J., Faircloth, B.C., Remm, M. et al. (2012) Primer3—new capabilities and interfaces. *Nucleic Acids Research*, *40*, e115.

Vandrisse, C.M. & Escalante-Semerena, J.C. (2016) New high-cloning-efficiency vectors for complementation studies and recombinant protein overproduction in *Escherichia coli* and *Salmonella enterica*. *Plasmid*, *86*, 1–6.

Weickert, M.J. & Adhya, S. (1992) A family of bacterial regulators homologous to gal and lac repressors. *The Journal of Biological Chemistry*, *267*, 15869–15874.

SUPPORTING INFORMATION

Additional supporting information can be found online in the Supporting Information section at the end of this article.

How to cite this article: Parks, A. R., McCormick, R. D., Byrne, J. A. & Escalante-Semerena, J. C. (2023). In *Salmonella enterica*, the pathogenicity island 2 (SPI-2) regulator PagR regulates its own expression and the expression of a five-gene operon that encodes transketolase C. *Molecular Microbiology*, *120*, 575–586. https://doi.org/10.1111/mmi.15143